NONCONVEX TOTAL VARIATION SPECKLED IMAGE RESTORATION VIA NONNEGATIVE QUADRATIC PROGRAMMING ALGORITHM

Paul Rodriguez

Digital Signal Processing Group, Pontificia Universidad Católica del Perú
Lima, Peru
phone: + (511) 626-2000 anx 4681, email: prodrig@pucp.edu.pe
web: http://sites.google.com/a/istec.net/prodrig

ABSTRACT

Within the TV framework there are several algorithms to restore images corrupted with Speckle (multiplicative) noise. Typically most of the methods convert the multiplicative model into an additive one by taking logarithms and can only handle the denoising case. By contrast, there are only a handful of algorithms that do not perform any conversion on the raw data and can handle the denoising and deconvolution cases, however their data fidelity term is non-convex.

In this paper, we present a flexible and computationally efficient method to restore speckled grayscale/color images via a non-convex multiplicative model. The proposed algorithm uses a quadratic approximation of the data fidelity term to pose the original problem as a non-negative quadratic programming problem. Our experimental results for the denoising and deconvolution cases shows that the reconstruction quality of the proposed algorithm outperforms state of the art algorithms for speckled image restoration and at the same time offers competitive computational performance.

1. INTRODUCTION

For images acquired via ultrasound, SAR (synthetic aperture radar) or coherent light imaging systems (e.g. Fabry-Perot interferometer, etc.), Speckle noise is a critical factor that limits their visual perception and processing (see [1, 2] among others). Typically, the multiplicative model

$$\mathbf{b} \quad = \quad (A\mathbf{u}^*)\cdot\boldsymbol{\zeta} \tag{1}$$

is considered, where A is a forward linear operator, $\mathbf{u}^*$ is the noise-free data and $\boldsymbol{\zeta}$ is the noise; also, it is assumed that $\mathbf{b},\mathbf{u}^* > 0$. Moreover, in the Speckle noise model, it is considered that $\boldsymbol{\zeta}$ follows the Gamma density

$$P_Z(\zeta) \quad = \quad \frac{L^L}{\Gamma(L)}\zeta^{L-1}\mathrm{e}^{-L\zeta} \tag{2}$$

with mean equal 1 and variance $1/L$.

While the focus of this paper is to restore speckled images using the Total Variation (TV) framework, we mention that there are several methods outside the TV framework: for instance, in [2] an extensive list of despeckle filtering algorithms is provided, which includes methods based on linear filtering (first-order statistics, local statistics, etc.), nonlinear filtering (median, linear scaling, etc.), diffusion filtering (anisotropic diffusion, etc.) and wavelet filtering.

Within the TV framework, there are several approaches to restore images corrupted with Speckle (multiplicative) noise. Typically most of the algorithms [3, 4, 5, 6, 7] convert the multiplicative model into an additive one by taking logarithms and can only handle the denoising case. To the best of our knowledge, there are only a handful of algorithms [8, 9, 10] that do not perform any conversion on the raw data and typically can handle the denoising and deconvolution cases (but not necessarily, e.g. [10] only addresses the denoising case), however their data fidelity term is non-convex.

In this paper we present a flexible and computationally efficient method to restore (denoise/deconvolve) speckled grayscale/color images. The proposed algorithm uses the non-convex multiplicative model introduced in [9]:

$$\begin{aligned} T(\mathbf{u}) \quad = \quad & \sum_k \frac{\mathbf{b}_k}{(A\mathbf{u})_k} + \log((A\mathbf{u})_k) + \\ & \frac{\lambda}{q}\left\| \sqrt{\sum_{n\in C}(D_x\mathbf{u}_n)^2 + (D_y\mathbf{u}_n)^2} \right\|_q^q \end{aligned} \tag{3}$$

where $n \in C = \{gray\}$, $q = 1$, $\mathbf{b}$ is the acquired image data (corrupted with Speckle noise), A is a forward linear operator, and $(A\mathbf{u})_m$ is the m-th element of $(A\mathbf{u})$ (full notation is described in Section 2); in [9] it was proved that (3) has a unique minimizer. While an artificial time marching approach was used to numerically solve the resulting Euler-Lagrange equation (from (3)) in [9], the proposed algorithm uses a second order Taylor approximation of the data fidelity term $F(\mathbf{u}) = \sum_k \frac{\mathbf{b}_k}{(A\mathbf{u})_k} + \log((A\mathbf{u})_k)$ to pose (3) as a Non-negative Quadratic Programming problem (NQP, see [11]) which can be solved with a similar approach as the IRN-NQP algorithm [12, 13]. The resulting algorithm has the following advantages:

- it is based on multiplicative updates only,
- has the ability to handle an arbitrary number of channels in (3), including the scalar (grayscale) and vector-valued (color) images ($C = \{r,g,b\}$ as special cases,
- most of its parameters are automatically adapted to the particular input dataset, and if needed, the norm of the regularization term (q in (3)) can be different than 1 ($0 < q \leq 2$).

2. TECHNICALITIES

We represent 2-dimensional images by 1-dimensional vectors: $\mathbf{u}_n$ ($n \in C$) is a 1-dimensional (column) or 1D vector that represents a 2D grayscale image obtained via any ordering (although the most reasonable choices are row-major or column-major) of the image pixel. For $C = \{r,g,b\}$ we have

that $\mathbf{u} = [(\mathbf{u}_r)^T(\mathbf{u}_g)^T(\mathbf{u}_b)^T]^T$ is a 1D (column) vector that represents a 2D color image.

The gradient and Hessian of the data fidelity term in (3) $F(u) = \sum_k \frac{\mathbf{b}_k}{(A\mathbf{u})_k} + \log((A\mathbf{u})_k)$ can be easily computed:

$$\nabla F(\mathbf{u}) = A^T\left(\frac{A\mathbf{u}-\mathbf{b}}{(A\mathbf{u})^2}\right) \quad (4)$$

$$\nabla^2 F(\mathbf{u}) = A^T \operatorname{diag}\left(\frac{2\mathbf{b}-A\mathbf{u}}{(A\mathbf{u})^3}\right) A, \quad (5)$$

and its quadratic approximation, $Q_F^{(k)}(\mathbf{u})$, can be written as

$$Q_F^{(k)}(\mathbf{u}) = F(\mathbf{u}^{(k)}) + \mathbf{g}^{(k)^T}\mathbf{v}^{(k)} + \frac{1}{2}\mathbf{v}^{(k)^T}H^{(k)}\mathbf{v}^{(k)} \quad (6)$$

where $\mathbf{v}^{(k)} = \mathbf{u} - \mathbf{u}^{(k)}$, $\mathbf{g}^{(k)} = \nabla F(\mathbf{u}^{(k)})$ and $H^{(k)} = \nabla^2 F(\mathbf{u}^{(k)})$. Note that (6) remains the same for color images ($n \in C = \{r,g,b\}$) and scalar operations applied to a vector are considered to be applied element-wise, so that, for example, $\mathbf{u} = \mathbf{v}^2 \Rightarrow u[k] = (v[k])^2$ and $\mathbf{u} = \frac{1}{\mathbf{v}} \Rightarrow u[k] = \frac{1}{v[k]}$.

Also, for the case of color images, the linear operator A in (3) is assumed to be decoupled, i.e. A is a diagonal block matrix with elements A_n; if A is coupled (inter-channel blur) due to channel crosstalk, it is possible to reduced it to a diagonal block matrix via a similarity transformation [14].

In the present work $\frac{1}{q}\left\|\sqrt{\sum_{n\in C}(D_x\mathbf{u}_n)^2 + (D_y\mathbf{u}_n)^2}\right\|_q^q$ is the generalization of TV regularization to color images ($n \in C = \{r,g,b\}$) with coupled channels (see [15, Section 9], also used in [16] among others), where we note that $\sqrt{\sum_{n\in C}(D_x\mathbf{u}_n)^2 + (D_y\mathbf{u}_n)^2}$ is the discretization of $|\nabla\mathbf{u}|$ for coupled channels (see [16, eq. (3)]), and D_x and D_y represent the horizontal and vertical discrete derivative operators respectively.

3. NON-CONVEX SPECKLE IRN-NQP ALGORITHM

In this section we succinctly describe previous works (within the TV framework) that tackle the problem of multiplicative noise removal. We continue to summarized the derivation of the non-convex Speckle IRN-NQP (Iteratively Reweighted Norm, non-negative quadratic programming) algorithm, where we also provide a brief description of the NQP [11] problem to finally list the proposed algorithm.

3.1 Previous Related Work

The first method within the TV framework devoted to restore images corrupted with Speckle noise was [8], which used a constrained optimization approach with two Lagrange multipliers; the denoising and deconvolution problems were addressed. In [3] the multiplicative model was converted into an additive one and used a multigrid algorithm to solve the resulting Euler-Lagrange equation. A framework based on MRF with levelable priors for restoration of images corrupted by Gaussian or Speckle (Rayleigh) was proposed in [4]; only the denoising problem was addressed. In [9] the data fidelity term was derived using (2) and the maximum a posteriori (MAP) criterion; an artificial time marching approach was used to numerically solve the resulting Euler-Lagrange equation; the denoising and deconvolution problems were addressed A general TV formulation was proposed in [5] which included several models ([8, 4, 9]) as special cases; it also replaced the regularizer TV(u) by TV(log u); only the denoising problem was addressed. In [6] the multiplicative model was converted into an additive one and used the split Bregman approach to solve the optimization problem; only the denoising problem was addressed. In [10] the non-convex model introduced in [9] was augmented with the Weberized TV as an extra regularizer and solved the Euler-Lagrange equation via a fixed-point iteration; only the denoising problem was addressed. A hard-thresholding of the curvelet transform of the log-image followed by a ℓ^1-TV in the log-image domain was used in [7]; only the denoising problem was addressed.

3.2 Non-negative Quadratic Programming (NQP)

Recently [11] an interesting and quite simple algorithm has been proposed to solve the NQP problem:

$$\min_{\mathbf{v}} \frac{1}{2}\mathbf{v}^T\Phi\mathbf{v} + \mathbf{c}^T\mathbf{v} \text{ s.t. } 0 \le \mathbf{v} \le \text{vmax}, \quad (7)$$

where the matrix Φ is assumed to be symmetric and positive defined, and vmax is some positive constant. The multiplicative updates for the NQP are summarized as follows (see [11] for details on derivation and convergence):

$$\Phi_{nl}^{+} = \begin{cases} \Phi_{nl} & \text{if } \Phi_{nl} > 0 \\ 0 & \text{otherwise} \end{cases} \text{ and } \Phi_{nl}^{-} = \begin{cases} |\Phi_{nl}| & \text{if } \Phi_{nl} < 0 \\ 0 & \text{otherwise,} \end{cases}$$

$$\mathbf{v}^{(k+1)} = \min\left\{\mathbf{v}^{(k)}\left[\frac{-\mathbf{c}+\sqrt{\mathbf{c}^2 + \boldsymbol{\upsilon}^{(k)}\boldsymbol{\nu}^{(k)}}}{2\boldsymbol{\upsilon}^{(k)}}\right], \text{vmax}\right\} \quad (8)$$

where $\boldsymbol{\upsilon}^{(k)} = \Phi^{+}\mathbf{v}^{(k)}$, $\boldsymbol{\nu}^{(k)} = \Phi^{-}\mathbf{v}^{(k)}$ and all algebraic operations in (8) are to be carried out element wise. The NQP is quite efficient and has been used to solve interesting problems such as statistical learning [11] among others.

3.3 Non-convex Speckle IRN-NQP Algorithm

Our aim is to express (3) as a quadratic functional in order to solve a NQP problem. First we note that after algebraic manipulation, $Q_F^{(k)}(\mathbf{u})$ (see (6)) can be written as

$$Q_F^{(k)}(\mathbf{u}) = \frac{1}{2}\mathbf{u}^T H^{(k)}\mathbf{u} + \mathbf{c}^{(k)}\mathbf{u} + \zeta_F, \quad (9)$$

where ζ_F is a constant with respect to $\mathbf{u}$, and $\mathbf{c}^{(k)} = \left(g^{(k)} - H^{(k)^T}\mathbf{u}^{(k)}\right) = A^T\left(\frac{2A\mathbf{u}^{(k)}-3\mathbf{b}}{(A\mathbf{u}^{(k)})^2}\right)$.

While not derived so here, the ℓ^q norm of the regularization term in (3) can be represented by a equivalent weighted ℓ^2 norm (see [12, 13] for details):

$$R^{(k)}(\mathbf{u}) = \frac{\lambda}{2}\left\|W_R^{(k)^{1/2}}D\mathbf{u}\right\|_2^2 + \zeta_R = \frac{\lambda}{2}\mathbf{u}^T D^T W_R^{(k)} D\mathbf{u}, \quad (10)$$

where ζ_R is a constant with respect to $\mathbf{u}$, I_N is a $N \times N$ identity matrix, $\otimes$ is the Kronecker product, $C = \{gray\}$, $N = 1$ or $C = \{r,g,b\}$, $N = 3$ and

$$D = I_N \otimes [Dx^T Dy^T]^T \quad W_R^{(k)} = I_{2N} \otimes \Omega^{(k)}, \tag{11}$$

$$\Omega^{(k)} = \text{diag}\left(\tau_{R,\varepsilon_R}\left(\sum_{n\in C}(D_x \mathbf{u}_n^{(k)})^2 + (D_y \mathbf{u}_n^{(k)})^2\right)\right). \tag{12}$$

Following a common strategy in IRLS type algorithms [17], the function

$$\tau_{R,\varepsilon_R}(x) = \begin{cases} |x|^{(q-2)/2} & \text{if } |x| > \varepsilon_R \\ \varepsilon_R^{(q-2)/2} & \text{if } |x| \le \varepsilon_R, \end{cases} \tag{13}$$

is defined to avoid numerical problems when $q < 2$ and $\sum_{n\in C}(D_x \mathbf{u}_n^{(k)})^2 + (D_y \mathbf{u}_n^{(k)})^2$ has zero-valued components.

Combining (9) and (10) we can write the quadratic approximation of (3) as (the constant terms are left out)

$$T^{(k)}(\mathbf{u}) = \frac{1}{2}\mathbf{u}^T\left(H^{(k)} + \lambda D^T W_R^{(k)} D\right)\mathbf{u} + \mathbf{c}^{(k)^T}\mathbf{u}, \tag{14}$$

to finally note that by using $\Phi^{(k)} = H^{(k)} + \lambda D^T W_R^{(k)} D$ and $\mathbf{c}^{(k)} = A^T\left(\frac{2A\mathbf{u}^{(k)} - 3\mathbf{b}}{(A\mathbf{u}^{(k)})^2}\right)$ we can iteratively solve (3) via (8).

Initialize

$\mathbf{u}^{(0)} = \mathbf{b}$

for $k = 0, 1, \ldots$

$$W_F^{(k)} = \text{diag}\left(\tau_{F,\varepsilon_F}\left(\frac{2\mathbf{b} - A\mathbf{u}^{(k)}}{(A\mathbf{u}^{(k)})^3}\right)\right), \; H^{(k)} = A^T W_F^{(k)} A$$

$$\Omega_R^{(k)} = \text{diag}\left(\tau_{R,\varepsilon_R}\left((D_x\mathbf{u}^{(k)})^2 + (D_y\mathbf{u}^{(k)})^2\right)\right)$$

$$W_R^{(k)} = \begin{pmatrix} \Omega_R^{(k)} & 0 \\ 0 & \Omega_R^{(k)} \end{pmatrix}$$

$$\Phi^{(k)} = H^{(k)} + \lambda D^T W_R^{(k)} D, \; \mathbf{c}^{(k)} = -A^T\left(\tau_{F,\varepsilon_F}\left(\frac{2A\mathbf{u}^{(k)} - 3\mathbf{b}}{(A\mathbf{u}^{(k)})^2}\right)\right)$$

$\mathbf{u}^{(k,0)} = \mathbf{u}^{(k)}$

$\varepsilon_{NQP}^{(k)} = \gamma \cdot 1\left(\frac{\|\Phi^{(k)}\mathbf{u}^{(k,0)} + \mathbf{c}^{(k)}\|_2}{\|\mathbf{c}^{(k)}\|_2}\right)^{\alpha}$ (NQP tolerance)

for $l = 0, 1, .., L$

$\boldsymbol{\upsilon}^{(k,l)} = \Phi^{+(k)}\mathbf{u}^{(k,l)}, \; \boldsymbol{\nu}^{(k,l)} = \Phi^{-(k)}\mathbf{u}^{(k,l)}$

$\mathbf{u}^{(k,l+1)} = \min\left\{\mathbf{u}^{(k,l)}\left[\frac{-\mathbf{c}^{(k)} + \sqrt{\mathbf{c}^{(k)^2} + \boldsymbol{\upsilon}^{(k,l)}\boldsymbol{\nu}^{(k,l)}}}{2\boldsymbol{\upsilon}^{(k,l)}}\right], \text{vmax}\right\}$

if $\left(\frac{\|\Phi^{(k)}\mathbf{u}^{(k,l+1)} + \mathbf{c}^{(k)}\|_2}{\|\mathbf{c}^{(k)}\|_2} < \varepsilon_{NQP}^{(k)}\right)$ **break;**

end

$\mathbf{u}^{(k+1)} = \mathbf{u}^{(k,l+1)}$

end

Algorithm 1: Non-convex Speckle IRN-NQP algorithm

It is easy to check that $\Phi^{(k)}$ is symmetric and positive define. Furthermore, we note that the proposed algorithm does not involve any matrix inversion: the fraction in the term $\mathbf{c}^{(k)} = A^T\left(\frac{2A\mathbf{u}^{(k)} - 3\mathbf{b}}{(A\mathbf{u}^{(k)})^2}\right)$ is a point-wise division (a check for zero must be performed to avoid numerical problems) as well as in the term $H^{(k)} = A^T \text{diag}\left(\frac{2\mathbf{b} - A\mathbf{u}^{(k)}}{(A\mathbf{u}^{(k)})^3}\right)A$;

Two other key aspects of the non-convex Speckle IRN-NQP algorithm is that it can auto-adapt the threshold value ε_R and that it includes the *NQP tolerance* ($\varepsilon_{NQP}^{(k)}$), used to terminate the inner loop in Algorithm 1 (see [13] for details). Experimentally, $\alpha \in [1\,..\,0.5]$, $\gamma \in$ [1e-3 .. 5e-1], and $L = 50$ give a good compromise between computational and reconstruction performance for the present work.

4. EXPERIMENTAL RESULTS

We compared the non-convex Speckle IRN-NQP algorithm with two state of the art methods: BF (Bioucas-Figueiredo [6]) and HXW (Huang-Xiao-Wei [10]). We note that for the denoising of greyscale images both [6, 10] report results, whereas for color images only [10] reports results. For the deconvolution case we only present results for the non-convex Speckle IRN-NQP algorithm, since to the best of our knowledge, the present paper is the only one that explicitly presents results for this case. We use the relative error and the peak signal-to-noise ratio (reErr = $\frac{\|\mathbf{u}-\mathbf{u}^*\|_2}{\|\mathbf{u}^*\|_2}$ and PSNR = $10\log_{10}\frac{\text{N}(\max\{\mathbf{u}^*\})^2}{\|\mathbf{u}-\mathbf{u}^*\|_2^2}$, respectively, N: total number of elements of $\mathbf{u}$, $\mathbf{u}$ is the observed/reconstructed image, $\mathbf{u}^*$ is the the original image and $\mathbf{u}^* \in [0, 1]$) as part of the reconstruction quality metrics to match the results presented in [6, 10]; we also provide the SNR and SSIM [18] metrics whenever appropriate.

(a) (b) (c)

Figure 1: Input test images: (a) Cameraman (grayscale) , (b) grayscale Lena and (c) color Lena. All images are 512×512.

All simulations have been carried out using Matlab-only code on a 1.73GHz Intel core i7 CPU (L2: 6144K, RAM: 6G). Results corresponding to the non-convex Speckle IRN-NQP algorithm presented here may be reproduced using the the NUMIPAD (v. 0.30) distribution [19], an implementation of IRN and related algorithms.

The test input images are greyscale Cameraman and Lena (Fig. 1a and 1b respectively) and color Lena (Fig. 1c). For the denoising cases Lena (grayscale and color) and Cameraman were corrupted with Speckle noise (generated according to (1)-(2)) with $L = 33$, 10, 5 and $L = 13$, 3 respectively, to match the experiments setup of [6, 10]. For the deconvolution case all the images were blurred by a 7×7 out-of-focus kernel (2D pill-box filter) and then corrupted with Speckle noise of similar characteristics as for the denoising case.

In Table 1 we summarized the results for the denoising case, where we show the ten-trial average of the SNR, SSIM, PSNR and reErr of the restore images for the non-convex IRN-NQP (10 outer loops with $L = 50$) and the BF (Bioucas-Figueiredo [6]) and HXW (Huang-Xiao-Wei [10]) algorithms (as respectively reported in [6] and [10]). The

Image	L	SNR		SSIM [18]		PSNR				reErr				Time (sec.)
		RAW	IRN-NQP	RAW	IRN-NQP	RAW	IRN-NQP	BF[(1)]	HXW [(2)]	RAW	IRN-NQP	BF[(1)]	HXW [(2)]	IRN-NQP
Lena	33	6.32	16.12	0.40	0.817	20.5	29.47	–	28.4	0.17	0.057	0.068	0.066	55.84
	10	1.10	13.63	0.26	0.719	15.2	27.45	–	23.6	0.30	0.077	–	–	73.90
	5	-1.89	11.72	0.18	0.662	12.3	25.83	–	–	0.40	0.097	0.113	0.115	83.92
Cam.	13	4.47	16.73	0.32	0.838	16.7	28.39	–	26.43	0.26	0.069	0.089	0.090	73.99
	3	-1.87	12.07	0.16	0.696	10.4	24.25	–	–	0.49	0.124	0.133	–	88.95
Lena (color)	33	7.60	18.16	–	–	20.3	30.86	–	29.93	0.17	0.052	–	0.075	161.98
	10	2.43	15.32	–	–	15.1	28.04	–	27.15	0.30	0.073	–	0.104	264.54
	5	-0.57	12.93	–	–	12.1	25.65	–	–	0.40	0.098	–	–	272.28

Table 1: Denoising case: Ten-trial average of the SNR, SSIM, PSNR and reErr of the restore images for the non-convex Speckle IRN-NQP (10 outer loops) algorithm and the BF (Bioucas-Figueiredo [6]) and HXW (Huang-Xiao-Wei [10]) algorithms. [(1)] Results are taken from [6, Table I]. [(2)] Results are taken from [10, Tables I and III]. See Figs. 2 and 3.

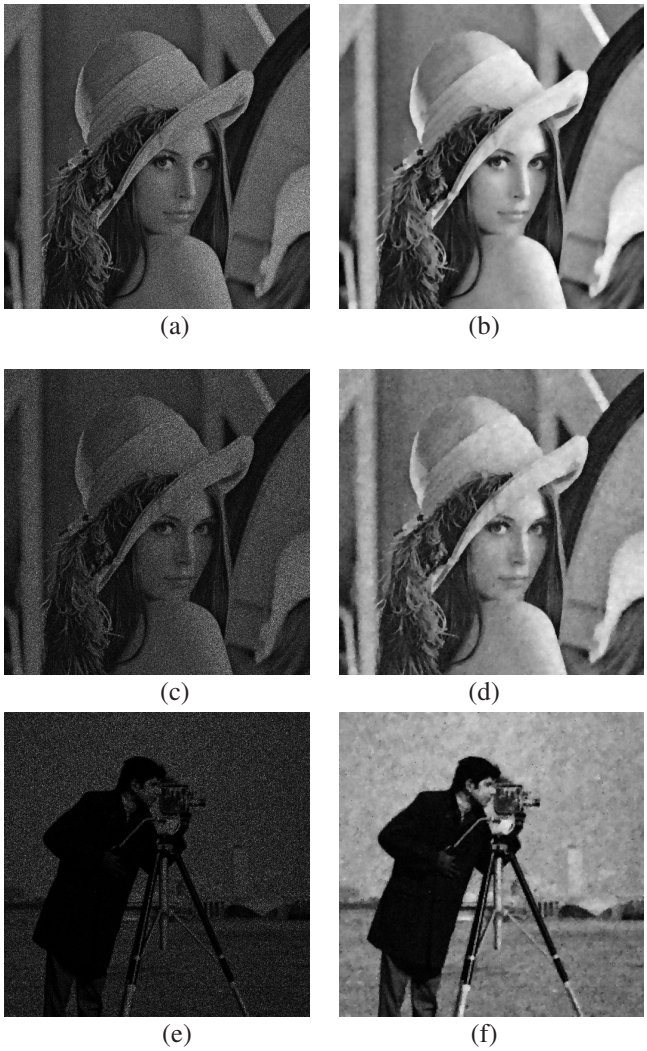

Figure 2: Speckled Lena with (a) L=33 (SNR=6.31dB), (c) L=10 (SNR=1.12dB) and Cameraman (e) with L=3 (SNR=−1.92dB), and denoised versions via the non-convex Speckle IRN-NQP algorithm (b) (SNR=16.12dB, PSNR=29.47dB, reErr=0.057), (c) (SNR=13.63dB, PSNR=27.45dB, reErr=0.077) and (f) (SNR=12.16dB, PSNR=24.19dB, reErr=0.121) respectively.

quality reconstruction of the proposed algorithm outperforms the BF and HXW for all cases. We also present the computational performance of our proposed algorithm in Table 1.

In Table 2 we summarized the results for the deconvolution case, where we show the ten-trial average of the SNR, SSIM, PSNR and reErr of the restore images for the non-convex IRN-NQP (8 outer loops, with $L = 50$). In Figs. 2, 3 and 4 we present the corrupted test images and their restored versions.

Image	L	SNR		SSIM [18]		PSNR		reErr		Time
		RAW	(*)	RAW	(*)	RAW	(*)	RAW	(*)	(sec.)
Lena	33	5.7	14.40	0.27	0.774	19.9	28.08	0.18	0.069	77.88
	10	0.9	13.37	0.18	0.717	15.1	27.07	0.30	0.078	90.97
	5	-2.0	12.21	0.14	0.699	12.26	25.75	0.41	0.091	96.41
Cam.	13	4.0	14.98	0.24	0.798	16.3	27.03	0.28	0.083	100.15
	3	-1.9	13.10	0.12	0.763	10.3	24.09	0.50	0.107	98.79
Lena (color)	33	7.0	15.66	–	–	19.7	29.17	0.18	0.069	278.93
	10	2.2	14.98	–	–	14.9	28.40	0.30	0.075	277.86
	5	-0.6	14.14	–	–	12.0	26.97	0.41	0.084	275.52

Table 2: Deconvolution case: Ten-trial average non-convex Speckle IRN-NQP[(*)] (8 outer loops) SNR, SSIM, PSNR and reErr of the restore images. See Fig. 4.

5. CONCLUSIONS

The reconstruction quality of the proposed algorithm outperforms state of the art algorithms [6, 10] for grayscale/color image denoising corrupted with Speckle noise. One of the main features of this recursive algorithm is that it is based on multiplicative updates only, and to best of our knowledge, the present paper is the only one that explicitly shows results for the deconvolution case. Furthermore, we are currently succesfully applying our method to denoise real-world Fabry-Perot fringes.

REFERENCES

[1] J. W. Goodman, "Some fundamental properties of speckle," *J. Opt. Soc. Am.*, vol. 66, no. 11, pp. 1145–1150, Nov 1976.

[2] C.. Loizou and C. Pattichis, *Despeckle Filtering Algorithms and Software for Ultrasound Imaging*, Synthesis Lectures on Algorithms and Software in Engineering. Morgan & Claypool Publishers, 2008.

[3] Chen Sheng, Yang Xin, Yao Liping, and Sun Kun, "Total variation-based speckle reduction using multi-grid

(a) (b) (c) (d)

Figure 3: Speckled color Lena (a) with L=33 (SNR=7.60dB), and (c) with L=10 (SNR=2.40) and denoised versions via the non-convex Speckle IRN-NQP algorithm (b) (SNR=18.16dB, PSNR=30.86dB, reErr=0.052) and (d) (SNR=15.32dB, PSNR=28.04dB, reErr=0.073) respectively.

(a) (b) (c) (d)

Figure 4: Blurred and speckled color Lena (a) with L=33 (SNR=7.00dB) and (c) with L=10 (SNR=2.30dB) and deconvolved versions via the non-convex IRN-NQP (b) (SNR=15.66dB, PSNR=29.17dB, reErr=0.069) and (d) (SNR=14.98dB, PSNR=28.40dB, reErr=0.075).

algorithm for ultrasound images," in *Image Analysis and Processing ICIAP 2005*, vol. 3617, pp. 245–252. Springer Berlin / Heidelberg, 2005.

[4] J. Darbon, M. Sigelle, and F. Tupin, "A note on nice-levelable MRFs for SAR image denoising with contrast preservation," Rapport interne ENST, 2006D006, Ecole Nat. Supérieure des Télécommunications, Paris, 2006.

[5] J. Shi and S. Osher, "A nonlinear inverse scale space method for a convex multiplicative noise model," *SIAM J. Img. Sci.*, vol. 1, pp. 294–321, September 2008.

[6] J. Bioucas and M. Figueiredo, "Total variation restoration of speckled images using a split-bregman algorithm," in *Proceedings of the International Conference on Image Processing (ICIP)*, 2009.

[7] S. Durand, J. Fadili, and M. Nikolova, "Multiplicative noise removal using l1 fidelity on frame coefficients," *Journal of Mathematical Imaging and Vision*, vol. 36, no. 3, pp. 201–226, 2010.

[8] S. Osher, N. Paragios, L. Rudin, and P. Lions, "Multiplicative denoising and deblurring: Theory and algorithms," in *Geometric Level Set Methods in Imaging, Vision, and Graphics*, pp. 103–119. Springer, 2003.

[9] G. Aubert, "A variational approach to remove multiplicative noise," *J. on Applied Mathematics*, vol. 68, no. 4, pp. 925–946, 2008.

[10] L. Huang, L. Xiao, and Z. Wei, "Multiplicative Noise Removal via a Novel Variational Model," *EURASIP Journal on Image and Video Processing*, vol. 2010, 2010, Article ID 250768.

[11] F. Sha, Y. Lin, L. Saul, and D. Lee, "Multiplicative updates for nonnegative quadratic programming," *Neural Comput.*, vol. 19, no. 8, pp. 2004–2031, 2007.

[12] P. Rodríguez and B. Wohlberg, "Efficient minimization method for a generalized total variation functional," *IEEE TIP*, vol. 18, no. 2, pp. 322–332, 2009.

[13] P. Rodríguez, "A non-negative quadratic programming approach to minimize the generalized vector-valued total variation functional," in *Proceedings of EUSIPCO'10*, Aalborg, Denmark, Aug. 2010.

[14] N. Galatsanos, A. Katsaggelos, T. Chin, and A. Hillery, "Least squares restoration of multichannel images," *IEEE TSP*, vol. 39, no. 10, pp. 2222–2236, 1991.

[15] A. Bonnet, "On the regularity of edges in image segmentation," *Annales de l'institut Henri Poincaré (C) Analyse non linéaire*, vol. 13, no. 4, pp. 485–528, 1996.

[16] X. Bresson and T. Chan, "Fast dual minimization of the vectorial total variation norm and applications to color image processing," *J. of Inverse Problems and Imaging*, vol. 2, no. 4, pp. 455–484, 2008.

[17] J. Scales and A. Gersztenkorn, "Robust methods in inverse theory," *Inverse Problems*, vol. 4, no. 4, pp. 1071–1091, Oct. 1988.

[18] Z. Wang, A. Bovik, H. Sheikh, and E. Simoncelli, "Perceptual image quality assessment: From error visibility to structural similarity," *IEEE T. on Image Processing*, vol. 13, no. 4, pp. 600–612, April 2004.

[19] P. Rodríguez and B. Wohlberg, "Numerical methods for inverse problems and adaptive decomposition (NUMIPAD)," `http://numipad.sourceforge.net/`.